0031-3998/05/5803-0568
PEDIATRIC RESEARCH
Vol. 58, No. 3, 2005
Printed in U.S.A.

Developmental Changes of Optical Properties in Neonates Determined by Near-Infrared Time-Resolved Spectroscopy

SONOKO IJICHI, TAKASHI KUSAKA, KENICHI ISOBE, KENSUKE OKUBO, KOU KAWADA, MASANORI NAMBA, HITOSHI OKADA, TOMOKO NISHIDA, TADASHI IMAI, AND SUSUMU ITOH

Department of Pediatrics [S.I., K.I., K.O., M.N., H.O., T.N., T.I., S.I.] and Maternal and Perinatal Center [T.K., K.K.], Faculty of Medicine, Kagawa University, Kitagun, Kagawa 761-0793, Japan

ABSTRACT

Near-infrared spectroscopy has been used for measurement of changes in cerebral Hb concentrations in infants to study cerebral oxygenation and hemodynamics. In this study, measurements by time-resolved spectroscopy (TRS) were performed in 22 neonates to estimate the values of light absorption coefficient and reduced scattering coefficient (μ'_s), cerebral Hb oxygen saturation (Sco_2), cerebral blood volume (CBV), and differential pathlength factor (DPF), and the relationships between postconceptional age and μ'_s, Sco_2, CBV, and DPF were investigated. A portable three-wavelength TRS system with a probe attached to the head of the neonate was used. The mean μ'_s values at 761, 795, and 835 nm in neonates were estimated to be (mean ± SD) 6.46 ± 1.21, 5.90 ± 1.15 and 6.40 ± 1.16/cm, respectively. There was a significant positive relationship between postconceptional age and μ'_s at those three wavelengths. The mean Sco_2 value was calculated to be 70.0 ± 4.6%, and postconceptional age and Sco_2 showed a negative linear relationship. The mean value of CBV was 2.31 ± 0.56 mL/100 g. There was a significant positive relationship between postconceptional age and CBV. The mean DPF values at 761, 795, and 835 nm were estimated to be 4.58 ± 0.41, 4.64 ± 0.46, and 4.31 ± 0.42, respectively. There was no relationship between postconceptional age and DPF at those three wavelengths. The results demonstrated that our near-infrared TRS method can be used to monitor μ'_s, Sco_2, CBV, and DPF in the neonatal brain at the bedside in an intensive care unit. (***Pediatr Res* 58: 568–573, 2005)**

Abbreviations

CBV, cerebral blood volume
DPF, differential pathlength factor
ICG, indocyanine green
NIRS, near-infrared spectroscopy
PLP, picosecond light pulser
Sco_2, cerebral Hb oxygen saturation
Spo_2, oxygen saturation by pulse oximeter
TRS, time-resolved spectroscopy
μa, light absorption coefficient
$\mu's$, light-reduced scattering coefficient

During the perinatal period, the brain undergoes anatomic, functional, and metabolic changes. The anatomic changes include neuronal proliferation, migration, organization, and myelination, and the metabolic changes match the process of initial overproduction and subsequent elimination of excessive neurons, synapses, and dendritic spines known to occur in the developing brain. Noninvasive assessment of cerebral anatomic changes and of oxygen delivery and utilization is useful for evaluating the effectiveness of therapy and for preventing oxygen toxicity in seriously ill neonates.

Near-infrared spectroscopy (NIRS) has been used in the clinical field with various measuring devices using several wavelengths. A method using continuous-wave NIRS has been developed and reported to be suitable for clinical use in infants (1–7). However, current commercially available NIRS systems can detect only changes in cerebral Hb. Because NIRS is based on the modified Beer-Lambert law, a change in hematocrit and blood volume as well as developmental and pathophysiologic changes in brain tissue affect the pathlength of near-infrared light. In a few recent studies, absolute values of cerebral Hb oxygen saturation (Sco_2) and cerebral blood volume (CBV) in infants were measured without inducing Hb concentration changes by using full-spectral near-infrared spectroscopy (8–11) and spatially resolved spectroscopy (12). However, these

Received February 13, 2004; accepted January 4, 2005.
Correspondence: Takashi Kusaka, M.D., Maternal and Perinatal Center, Faculty of Medicine, Kagawa University, Mikicho 1750-1, Kitagun, Kagawa 761-0793, Japan; e-mail: kusaka@kms.ac.jp.
Supported by grants-in-aid for scientific research 17390307, 16591075, 15591158, and 15591159, from the Ministry of Education, Culture, Sports, Science and Technology of Japan.

DOI: 10.1203/01.PDR.0000175638.98041.0E

devices can measure only light absorption coefficient (μ_a), which represents the physiologic state, particularly the Hb concentration and oxygen saturation.

A recently developed time-resolved spectroscopy (TRS) device enables simultaneously quantitative analysis of μ_a and light-reduced scattering coefficient (μ'_s) in tissue by using the photon diffusion theory. μ'_s is thought to be a new parameter for assessment of structural changes in the brain, such as brain edema and myelination. Although TRS has been used in neonates, there have only been a few reports on its use in neonates, and measurements in neonates at the bedside have not been possible because of the size and the cost of typical laboratory equipment needed for these measurements. However, a new TRS device that is portable and has a high data acquisition rate was used clinically recently. This TRS system can be used *1*) for continuous absolute quantification of hemodynamic variables and *2*) for better estimation of light-scattering properties by measurement of μ'_s and differential pathlength factor (DPF). The aim of this study was to measure the values of μ'_s, μ_a, Sco_2, CBV, and DPF in neonates using TRS and to determine the relationships between postconceptional age and μ'_s, Sco_2, CBV, and DPF.

METHODS

Patient population. Measurements were carried out in 27 neonates who were undergoing neonatal intensive care at the Maternal and Perinatal Center of Kagawa University Hospital. Written informed consent was obtained from the parents of each neonate. The study was also approved by a local ethics committee. Data from five neonates were excluded from the analysis because the measurements were affected by movement artifacts. Successful measurements were performed in 22 neonates. Their gestational age (mean ± SD) was 36.8 ± 3.1 wk, and birth weight was 2365 ± 791 g. The mean time after birth when measurements were carried out was 32.9 ± 21.1 h. The clinical diagnosis of each neonate is shown in Table 1. Mechanical ventilation was required in four neonates, and three neonates received catecholamines during this study. No neonates have problems in their prognosis at present.

Near-infrared time-resolved spectroscopy system and analysis. We used a portable three-wavelength TRS system (TRS-10; Hamamatsu Photonics K.K., Hamamatsu, Japan) and attached a probe to the forehead of each neonate. In the TRS system, a time-correlated single-photon-counting technique is used for detection. The system is controlled by a computer through a digital I/O interface that consists of a three-wavelength (761, 795, and 835 nm) picosecond light pulser (PLP) as the pulse light source, a photon-counting head for single photon detection, and signal-processing circuits for time-resolved measurement. The PLP emits NIR light with a pulse duration of ~100 ps and an average power of at least 150 μW at each wavelength at repetition of 5 MHz. The input light power to the patient was ~20 μW.

The light from the PLP is sent to a patient by a source fiber with a length of 3 m, and the photon re-emitted from the patient is collected simultaneously by a detector fiber bundle with a length of 3 m (13). The light source fiber used in this study was a graded-index-type single fiber with a numerical aperture of 0.25 and a core diameter of 200 μm, and the light detector fiber was a bundle fiber with a diameter of 3 mm and numerical aperture of 0.21. Finally, a set of histograms of photon flight time, which is called a re-emission profile, is recorded (14,15). One temporal re-emission profile includes 1024 time channels that span ~10 ns with a time step of ~10 ps. In this study, the emerging light was collected over a period of 1 s to exceed at least 1000 count of photon at the peak channel of the re-emission profiles. The instrumental response was measured with the input fiber placed opposite the receiving fiber through a neutral density filter. The instrumental response of the TRS system was ~150 ps Full-Width Half-Maximum at each wavelength.

The re-emission profiles observed at each measurement point were fitted by the photon diffusion equation proposed by Patterson *et al.* (16) to calculate the values of μ_a and μ'_s of the head at wavelengths of 761, 795, and 835 nm. In the fitting procedure, a nonlinear least squares fitting method based on Levenberg-Marquardt's method was used. In each iterative calculation, the function from the photon diffusion equation in reflectance mode, which was convoluted with the instrumental response, was fitted to the observed re-emission profile. The calculation regions were determined to include the observed profile data, and data of 600 channels were included into the fit.

Table 1. *Clinical details*

Neonate no.	Gestational age (wk)	Birth weight (g)	Clinical diagnosis
1	30.1	1531	RDS, MV
2*	32.1	2106	RDS, MV
3*	33.1	1999	Congenital pneumonia, PPHN, MV
4	33.4	1940	TTN
5	34.6	1280	RDS, SGA
6*	35	733	RDS, MV, anemia, SGA
7	35	2222	TTN
8	35.1	2377	TTN
9	35.7	1714	Fetal arrhythmia, SGA
10	36.7	1857	Maternal SLE, light for gestational age
11	37	2763	Hypoglycemia
12	37.4	1908	Light for gestational age
13	37.6	1571	Maternal SLE, SGA
14	37.7	2323	Light for gestational age
15	38.6	2764	Twin A, healthy neonate
16	38.6	2736	Twin B, healthy neonate
17	39.1	3094	Healthy neonate
18	39.6	3426	Healthy neonate
19	40.3	3506	First branchial arch syndrome
20	40.6	3184	Meconium aspiration syndrome
21	41.3	3422	Healthy neonate
22	41.7	3580	Meconium aspiration syndrome
Mean	36.8	2365	
SD	3.1	791	

RDS, respiratory distress syndrome; MV, mechanical ventilation; PPHN, persistent pulmonary hypertension of the newborn; TTN, transient tachypnea of the newborn; SGA, small for gestational age; SLE, systemic lupus erythematosus.

* These infants had catecholamines.

After determination of the values of μ_a at three wavelengths, the oxyHb and deoxyHb concentrations were calculated from the absorption coefficients of oxyHb and deoxyHb using the following equations with the assumption that background absorption is due only to 85% (by volume) water (8):

$$\mu_{a\,761nm} = \epsilon^{oxyHb}_{761nm}\,[oxyHb] + \epsilon^{deoxyHb}_{761nm}\,[deoxyHb] + \epsilon^{water}_{761nm}\,[water\ volume\ fraction]$$

$$\mu_{a\,795nm} = \epsilon^{oxyHb}_{795nm}\,[oxyHb] + \epsilon^{deoxyHb}_{795nm}\,[deoxyHb] + \epsilon^{water}_{795nm}\,[water\ volume\ fraction]$$

$$\mu_{a\,835nm} = \epsilon^{oxyHb}_{835nm}\,[oxyHb] + \epsilon^{deoxyHb}_{835nm}\,[deoxyHb] + \epsilon^{water}_{835nm}\,[water\ volume\ fraction]$$

In these equations, $\epsilon^{X}_{\lambda nm}$ is the extinction coefficient at λ nm, and [oxyHb] and [deoxyHb] are concentration of oxyHb and deoxyHb, respectively.

First, water absorption was subtracted from μ_a at each of the three wavelengths, and then the concentrations of oxyHb and deoxyHb were estimated using the least squares fitting method. The absorption coefficients for oxyHb, deoxyHb, and water shown in Table 2 were used.

Cerebral total Hb (totalHb) concentration, Sco_2, and CBV were calculated as follows:

$$[totalHb] = [oxyHb] + [deoxyHb],$$
$$ScO_2(\%) = \{[oxyHb]/([oxyHb] + [deoxyHb])\} \times 100,$$
$$CBV\ (ml/100g) = [totalHb] \times MW_{Hb} \times 10^{-6}/(tHb \times 10^{-2} \times D_t \times 10),$$

where [ ] indicates Hb concentration (μM), MW_{Hb} is the molecular weight of Hb (64,500), tHb is venous Hb concentration (g/dL), and D_t is brain tissue density (1.05 g/mL).

Table 2. *Absorption coefficients for oxyHb, deoxyHb, and water*

	oxyHb (mM/cm)	deoxyHb (mM/cm)	water (cm)
761 nm	1.418	3.841	0.0272
795 nm	1.919	2.016	0.0214
835 nm	2.487	1.798	0.0358

The mean pathlength was calculated from the difference between the center of gravity of the measured reemission profile and that of the instrumental function. We assumed that the value for the refractive index of brain tissue is 1.4 (17). The ratio of optical pathlength to interoptode distance is defined as the DPF (18).

All of the neonates were in the supine position during measurements. Their condition was stable, and they were sleeping during the procedure at least 12 min. The optode positions were on the forehead of each neonate, and interoptode space was 26–32 mm. At the same time, oxygen saturation by pulse oximeter (Spo_2) was monitored using a Nellcor N550 (Tyco, Tokyo, Japan).

The average values of μ'_s, Sco_2, CBV, and DPF for each patient were calculated for a period of 5 min during the 12-min measurement period in a steady state not affected by movement artifacts. Variation, particularly in cerebral oxygen delivery, can occur over short periods, and long averaging measurement time is needed. Sco_2 depends on cerebral oxygen delivery and extraction, both of which vary with postconceptional age and postnatal age. We previously reported postnatal changes in CBV and Sco_2 in normal infants determined by full-spectrum NIRS. CBV and Sco_2 changed within the first 15 min after birth (10,11), but remained constant from 12 h after birth until day 5 (9). In the present study, the average time at which measurements were carried out after birth was 33 ± 21 h, and the values of Sco_2 and CBV in this study therefore were not affected by birth stress. In a previous study, the cerebral blood velocity in infants measured by Doppler ultrasound showed cyclical fluctuations with frequency ranging from 1.5 to 5 cycles/min (19). NIRS studies have also shown oscillations of the Hb oxygenation state with frequency ranging from 3 to 5 cycles/min (20). Therefore, the use of average values for a period of 5 min in each neonate in this study seems sufficient for estimation of cerebral Hb in a steady state.

Statistical analysis. A StatView-J 5.0 package for the Macintosh computer was used for statistical analysis. The level of statistical significance was set at a probability of $p < 0.05$ for all tests. All measurement results are expressed as means ± SDs.

RESULTS

The values of DPF, μ_a, μ'_s, Sco_2, totalHb, and CBV are shown in Table 3. The values of μ'_s in the 22 neonates at 761, 795, and 835 nm were estimated to be (mean ± SD) 6.46 ± 1.21, 5.90 ± 1.15, and 6.40 ± 1.16/cm, respectively. As shown in Fig. 1, there was a significant positive relationship between postconceptional age and μ'_s at the three wavelengths.

Mean Sco_2 was 70.0 ± 4.6% (range 60.8–78.8%), and mean Spo_2 was 98.6% (range 92–100%). Postconceptional age and Sco_2 showed a significant negative linear relationship as shown in Fig. 2.

There was a significant positive relationship between postconceptional age and cerebral totalHb. The relationship between postconceptional age and cerebral totalHb was $y = 4.23x + 91.9$ ($r = 686$, $p < 0.001$). The mean CBV was 2.31 ± 0.56 mL/100 g (range 1.42–3.40 mL/100 g). As shown in Fig. 3, there was a significant positive relationship between postconceptional age and CBV. There was no relationship between blood Hb concentration and CBV.

The DPF values at 761, 795, and 835 nm were estimated to be 4.58 ± 0.41, 4.64 ± 0.46, and 4.31 ± 0.42, respectively. There was no relationship between postconceptional age and DPF at any of the three wavelengths.

DISCUSSION

This is the first report on the relationship between postconceptional age and μ'_s in the neonatal brain. We previously reported that there were no significant differences between the values of μ'_s at each wavelength for inspired fractional O_2 levels in the range of 4–100% in a piglet hypoxia model. These results are similar to those obtained in a study by Zhang *et al.* (21) showing that scattering changes detected by frequency-domain spectroscopy were associated only with asphyxia and death. Yamashita *et al.* (22) reported the results of a preliminary study on μ'_s in the piglet brain by using TRS. Their

Table 3. *Results of the study*

Neonate no.	Interoptode spacing (cm)	DPF			μa (/cm)			μ's (/cm)			Cerebral total Hb (μM)	Sco_2 (%)	Blood Hb (g/dL)	CBV (mL/100 g)
		761 nm	795 nm	835 nm	761 nm	795 nm	835 nm	761 nm	795 nm	835 nm				
1	3.1	3.91	4.05	3.76	0.11	0.09	0.12	3.69	3.61	3.83	39.7	73.1	16.5	1.48
2	3	5.09	5.12	4.69	0.13	0.12	0.16	6.37	6.29	6.46	54.2	78.8	15	2.22
3	2.6	5.20	5.37	4.91	0.11	0.10	0.13	6.43	6.3	6.46	41.6	71.3	14	1.82
4	3.2	4.71	4.48	4.39	0.11	0.08	0.13	5.19	3.89	4.98	39.3	67.2	17	1.42
5	2.8	4.32	4.37	3.84	0.17	0.16	0.19	6.15	6.07	5.48	70.4	72	18.8	2.30
6	2.9	4.47	4.76	4.31	0.12	0.10	0.12	5.07	5.01	4.86	41.3	65	9.7	2.61
7	2.6	4.81	4.81	4.39	0.13	0.11	0.15	6.09	5.63	5.97	51	75.4	14	2.24
8	2.8	5.06	5.29	4.76	0.13	0.12	0.15	6.64	6.62	6.53	50.1	71.2	18.6	1.65
9	2.6	3.88	3.85	3.10	0.17	0.16	0.21	5.26	5.01	5.19	77	74.9	23.1	2.05
10	3.2	4.36	4.54	4.14	0.16	0.14	0.18	5.77	5.65	5.71	64	70.2	22.3	1.76
11	2.7	4.84	4.97	4.60	0.13	0.11	0.15	6.27	5.91	6.26	49.6	69.3	16.8	1.81
12	2.8	4.25	4.12	4.07	0.17	0.13	0.20	5.97	4.6	6.16	69.6	66.4	20	2.14
13	2.8	4.02	3.87	3.94	0.17	0.14	0.23	5.4	4.48	6.46	81.8	75.8	15.8	3.18
14	3.2	4.63	4.65	4.20	0.15	0.14	0.17	7.10	6.67	6.65	72.5	73.8	17.9	2.49
15	3.1	5.02	5.18	4.74	0.17	0.14	0.17	7.62	7.11	7.13	63.0	64.7	15.6	2.48
16	3	4.95	5.11	4.66	0.14	0.12	0.15	6.76	6.35	6.39	53.8	65.8	16	2.07
17	3	4.66	4.72	4.38	0.18	0.16	0.20	7.13	6.65	6.84	72.2	68.4	20	2.22
18	2.7	4.34	4.49	4.15	0.21	0.17	0.21	8.53	7.79	7.84	90.5	62.5	18.8	2.96
19	2.8	4.34	4.30	4.21	0.27	0.22	0.30	8.65	7.39	9.09	114.6	71.2	20.7	3.40
20	3	3.99	4.02	4.08	0.20	0.16	0.24	6.06	5.03	6.98	83.4	72.4	17.6	2.91
21	3	4.84	4.93	4.50	0.19	0.17	0.21	8.08	7.56	7.59	78.7	68.7	19.1	2.53
22	2.7	5.03	4.99	4.89	0.16	0.12	0.18	7.85	6.18	7.99	65.7	60.8	12.9	3.13
Mean	2.9	4.58	4.64	4.31	0.16	0.13	0.18	6.46	5.90	6.40	64.7	70.0	17.3	2.31
SD	0.2	0.41	0.46	0.42	0.04	0.03	0.04	1.21	1.15	1.16	18.9	4.6	3.1	0.56

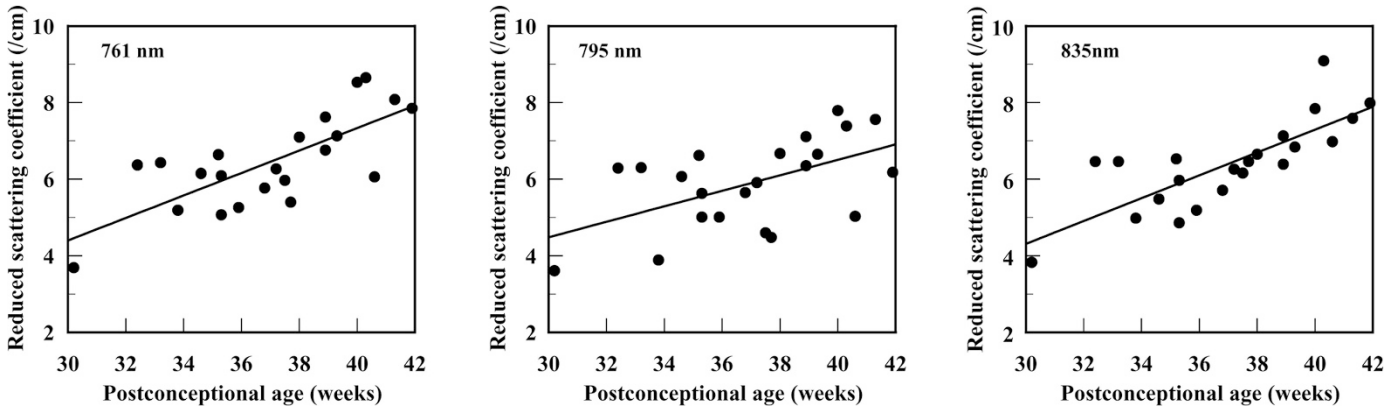

Figure 1. Relationships between postconceptional age and μ'_s at 761, 795, and 835 nm in 22 neonates. The relationships between postconceptional age and μ'_s at 761, 795, and 835 nm were $y_{761\ nm} = 0.293x - 4.40$ ($r = 0.742$, $p < 0.001$), $y_{795\ nm} = 0.202x - 1.58$ ($r = 0.539$, $p = 0.010$), and $y_{835\ nm} = 0.298x - 4.65$ ($r = 0.787$, $p < 0.001$), respectively.

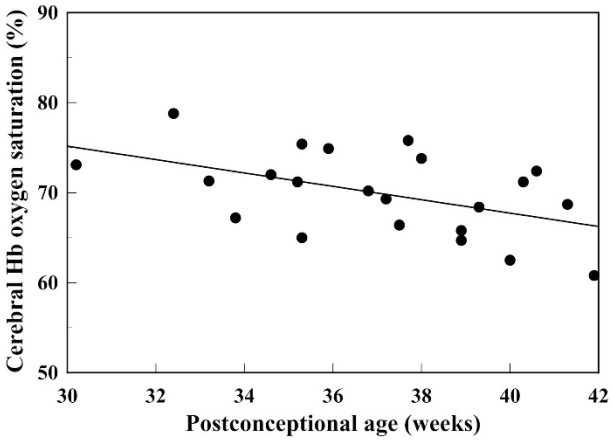

Figure 2. Relationships between postconceptional age and cerebral Hb oxygen saturation in 22 neonates. The relationship between postconceptional age and cerebral Hb oxygen saturation was $y = -0.74x + 97.5$ ($r = -0.498$, $p = 0.018$).

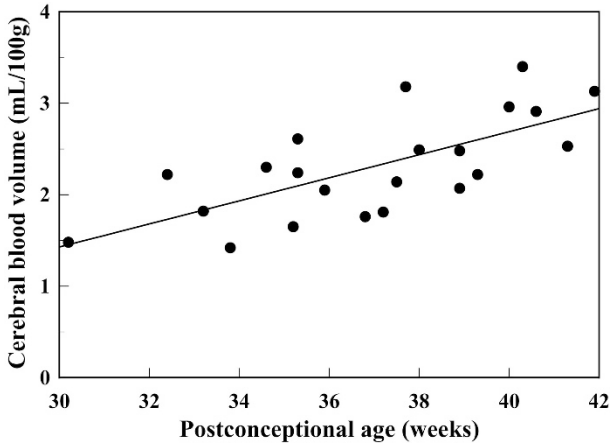

Figure 3. Relationships between postconceptional age and CBV in 22 neonates. The relationship between postconceptional age and CBV was $y = 0.126x - 2.352$ ($r = 0.696$, $p < 0.001$).

results showed a notable decrease after death. Tissue edema and structural changes occur during severe hypoxia, particularly at and after death, and values of μ'_s are thought to change only during structural changes in tissue as a result of cerebral energy failure. Furthermore, developmental changes in the brain, especially neuronal proliferation, migration, organization, and myelination, were thought to be related to the positive relationship between μ'_s and postconceptional age. However, at present, magnetic resonance imaging techniques enable a much better assessment of anatomic development in infants.

Values of Sco_2 in infants that were obtained in previous studies using NIRS (8–12,23,24) are summarized in Table 4. Mean Sco_2 in the 22 neonates in this study was 70.0 ± 4.6%, and the range of Sco_2 values was small (60.8–78.8%). This range is similar to those previously reported (63–69%) in infants (8–12,23). Results of measurements using the TRS system also showed a decrease in Sco_2 with increasing postconceptional age. Sco_2 measured by NIRS represents a mixed vascular Hb oxygen saturation of capillaries, arteriae, and veins in that tissue field. Absolute measurements are made on the basis of the assumption of homogeneity of tissue. The reason for decrement of Sco_2 with increasing postconceptional age is that cerebral Hb oxygen consumption increases with advance of postconceptional age, and this leads to a decrease in venous Hb oxygen saturation. The lower values of cerebral oxygen consumption in neonates than in older children is likely to be due to changes in the structural complexity and functional activity of the brain that occur across the range of gestational ages (25–27). Another reason is that venous structural change in the brain surface occurs in this period. The ratio of venous to arterial vessels may increase, and this would lead to an increase in cerebral content of deoxyHb and therefore to decrease in Sco_2.

In this study, we noninvasively estimated values of CBV in neonates using a TRS system. Brazy *et al.* (1,28) monitored changes in CBV in infants, but quantification of CBV has not been possible. Methods for calculating CBV using oxyHb as a tracer with continuous-wave NIRS have been reported (29,30). Moreover, without changing oxyHb, CBV has been measured using indocyanine green (ICG) with spatially resolved NIRS (31). However, to our knowledge, there have been no studies in which CBV in infants was estimated by using a TRS system without changes in oxyHb or without using ICG injection. The mean value obtained in the neonates in the present study, 2.31 ± 0.56 mL/100 g, is similar to the values estimated in infants

Table 4. *Some values of Sco_2 in infants using NIRS*

Methods	Subjects	Age (wk)	Mean Sco_2 (%)	Materials	References
FSS*	1		63		8
FSS	15	38 ± 2	68	Term neonates	9
FSS	7	36–41	69		10
FSS	20	37–41	66	Vaginal delivery	11
	6	37–41	57	Cesarean section	
CW	40	<32	67	Preterm infants	23
FD	20	0 mo–6 y	53	Congenital heart disease	24
SRS	15	<31	66	Preterm neonates	12
TRS	22	30–42	70		Present study

FSS, full-spectral spectroscopy; CW, continuous wave spectroscopy; FD, frequency domain spectroscopy; SRS, spatially resolved spectroscopy.
* Water reference method.

by using the continuous-wave NIRS method with changes in arterial Hb saturation (2.2–3.0 mL/100 g) (29) and with changes in Pco_2 (3.7 mL/100 g) (30). These values in infants all are lower than those estimated in human adults using singe photon emission computed tomography (4.8 ± 0.4 mL/100 g) (32) and using positron emission tomography (4.7 ± 1.1 mL/100 g) (33). The reason for smaller values of CBV in neonates than in adults is that regional CBV is smaller in white cerebral matter than in gray cerebral matter, and the relatively low mean CBV may reflect a relative preponderance of white matter compared with that in the adult brain (29). In this study, the values of CBV increased with advance of postconceptional age. This relationship between postconceptional age and CBV is based on the results of an anatomic study of cerebral blood vessels showing that the percentage of blood vessel area in gray matter and white matter increased as a function of gestational age (34). Indeed, the CBV value estimated by using spatially resolved NIRS with ICG (1.72 ± 0.76 mL/100 g) was smaller than that obtained in our study, because the gestational age of the subjects in that study (mean gestational age 28 wk; mean postnatal age 6 d) was less than that of our patients (31).

DPFs at 761, 795, and 835 nm were estimated to be 4.58 ± 0.41, 4.64 ± 0.46, and 4.31 ± 0.42, respectively. Various experimental techniques have been used to determine DPF in infants. These are based on measurements of absorption of light by time-of-flight spectroscopy (35,36), phase-resolved spectroscopy (26,37), or the water peak method (8). The mean value of DPFs estimated by using time-of-flight spectroscopy at 783 nm in postmortem infants has been reported to be 4.39 ± 0.28 ($n = 6$) (35) and 3.85 ± 0.57 ($n = 10$) (36). Duncan *et al.* (26,37) measured DPFs in a group of 35 infants using phase-resolved spectroscopy and calculated the mean values to be 5.11 ± 0.48 at 744 nm and 4.67 ± 0.65 at 832 nm. DPFs that were calculated by the water peak method at 730 nm and 830 nm were 4.66 ± 1.01 and 3.91 ± 0.75, respectively (8). The DPF values obtained in this study are similar to those obtained in the group of infants using phase-resolved spectroscopy.

The sensitivity and the reliability of our TRS method were previously assessed by using an *in vitro* model and a piglet hypoxia model. In the *in vitro* study, the use of intralipids and a blood phantom showed that qualitative measurements of Hb concentrations and of oxygen saturation could be made under the same conditions as those in an *in vivo* study. In the piglet hypoxia model, the mean Sco_2 value at normoxia was calculated to be 62%, and the contributions of arterial blood and venous blood were estimated to be 41 and 59%, respectively (38). The ratio of the contribution of arterial blood to that of venous blood obtained in the study using a piglet hypoxia model is almost the same as the ratio reported by Brun *et al.* (39) and by Kusaka *et al.* (40). The results of the present study demonstrated that our TRS method can be used to monitor Sco_2 and CBV. However, the number of such neonates in this study was too small for us to reach any definite conclusion, and further study is required.

In conclusion, the results of this study confirm that the new TRS is a practical method for measurements of μ'_s, Sco_2, CBV, and DPF in neonates at the bedside in an intensive care unit.

REFERENCES

1. Brazy JE, Lewis DV, Mitnick MH, Jobsis van der Vliet FF 1985 Noninvasive monitoring of cerebral oxygenation in preterm infants: preliminary observations. Pediatrics 75:217–225
2. Wyatt JS, Cope M, Delpy DT, Wray S, Reynolds EO 1986 Quantification of cerebral oxygenation and haemodynamics in sick newborn infants by near infrared spectrophotometry. Lancet 2:1063–1066
3. Edwards AD, Wyatt JS, Richardson C, Delpy DT, Cope M, Reynolds EO 1988 Cotside measurement of cerebral blood flow in ill newborn infants by near infrared spectroscopy. Lancet 2:770–771
4. Liem KD, Hopman JC, Oeseburg B, de Haan AF, Festen C, Kollee LA 1995 Cerebral oxygenation and hemodynamics during induction of extracorporeal membrane oxygenation as investigated by near infrared spectrophotometry. Pediatrics 95:555–561
5. Pryds O, Greisen G, Skov LL, Friis-Hansen B 1990 Carbon dioxide-related changes in cerebral blood volume and cerebral blood flow in mechanically ventilated preterm neonates: comparison of near infrared spectrophotometry and 133Xenon clearance. Pediatr Res 27:445–449
6. van Bel F, Dorrepaal CA, Benders MJ, Zeeuwe PE, van de Bor M, Berger HM 1993 Changes in cerebral hemodynamics and oxygenation in the first 24 hours after birth asphyxia. Pediatrics 92:365–372
7. Tyszczuk L, Meek J, Elwell C, Wyatt JS 1998 Cerebral blood flow is independent of mean arterial blood pressure in preterm infants undergoing intensive care. Pediatrics 102:337–341
8. Cooper CE, Elwell CE, Meek JH, Matcher SJ, Wyatt JS, Cope M, Delpy DT 1996 The noninvasive measurement of absolute cerebral deoxyhemoglobin concentration and mean optical path length in the neonatal brain by second derivative near infrared spectroscopy. Pediatr Res 39:32–38
9. Kusaka T, Isobe K, Kawada K, Ohtaki Y, Itoh S, Hirao K, Onishi S 1998 Postnatal changes in the cerebral oxygenation in normal and asphyxiated neonates. Proc SPIE Int Soc Opt Eng 3194:92–102
10. Isobe K, Kusaka T, Fujikawa Y, Kondo M, Kawada K, Yasuda S, Itoh S, Hirao K, Onishi S 2000 Changes in cerebral hemoglobin concentration and oxygen saturation immediately after birth in the human neonate using full-spectrum near infrared spectroscopy. J Biomed Opt 5:283–286
11. Isobe K, Kusaka T, Fujikawa Y, Okubo K, Nagano K, Yasuda S, Kondo M, Itoh S, Hirao K, Onishi S 2002 Measurement of cerebral oxygenation in neonates after vaginal delivery and cesarean section using full-spectrum near infrared spectroscopy. Comp Biochem Physiol A Mol Integr Physiol 132:133–138
12. Naulaers G, Morren G, Van Huffel S, Casaer P, Devlieger H 2002 Cerebral tissue oxygenation index in very premature infants. Arch Dis Child Fetal Neonatal Ed 87:F189–F192

13. Liebert A, Wabnitz H, Grosenick D, Macdonald R 2003 Fiber dispersion in time domain measurements compromising the accuracy of determination of optical properties of strongly scattering media. J Biomed Opt 8:512–516
14. Kusaka T, Hisamatsu Y, Kawada K, Okubo K, Okada H, Namba M, Imai T, Isobe K, Itoh S 2003 Measurement of cerebral optical pathlength as a function of oxygenation using near-infrared time-resolved spectroscopy in a piglet model of hypoxia. Opt Rev 10:466–469
15. Oda M, Yamashita Y, Nakano T, Suzuki A, Shimizu K, Hirano I, Shimomura F, Ohmae E, Suzuki T, Tsuchiya Y 1999 Near infrared time-resolved spectroscopy system for tissue oxygenation monitor. Proc SPIE Int Soc Opt Eng 3597:611–617
16. Patterson MS, Chance B, Wilson B 1989 Time resolved reflectance and transmittance for the non-invasive measurement of optical properties. Appl Opt 289:2331–2336
17. Bolin PF, Preuss LE, Taylor RC, Ference RJ 1989 Refractive index of some mammalian tissues using a fiber optic cladding method. Appl Opt 28:2297–2303
18. Delpy DT, Cope M, van der Zee P, Arridge S, Wray S, Wyatt J 1988 Estimation of optical pathlength through tissue from direct time of flight measurement. Phys Med Biol 33:1433–1442
19. Anthony MY, Evans DH, Levene MI 1991 Cyclical variations in cerebral blood flow velocity. Arch Dis Child 66:12–16
20. Taga G, Konishi Y, Maki A, Tachibana T, Fujiwara M, Koizumi H 2000 Spontaneous oscillation of oxy- and deoxy-hemoglobin changes with a phase difference throughout the occipital cortex of newborn infants observed using non-invasive optical topography. Neurosci Lett 282:101–104
21. Zhang G, Katz A, Alfano RR, Kofinas AD, Kofinas DA, Stubblefield PG, Rosenfeld W, Beyer D, Maulik D, Stankovic MR 2000 Brain perfusion monitoring with frequency-domain and continuous-wave near-infrared spectroscopy: a cross-correlation study in newborn piglets. Phys Med Biol 45:3143–3158
22. Yamashita Y, Oda M, Naruse H, Tamura M 1996 In vivo measurement of reduced scattering and absorption coefficients of living tissue using time-resolved spectroscopy. In: Alfano RR, Fujimoto GJ (eds) OSA TOPS on Advances in Optical Imaging and Photon Migration, Optical Society of America, Washington, D.C., Vol 2. pp 387–390
23. Dani C, Bertini G, Reali MF, Tronchin M, Wiechmann L, Martelli E, Rubaltelli FF 2000 Brain hemodynamic changes in preterm infants after maintenance dose caffeine and aminophylline treatment. Biol Neonate 78:27–32
24. Watzman HM, Kurth CD, Montenegro LM, Rome J, Steven JM, Nicolson SC 2000 Arterial and venous contributions to near-infrared cerebral oximetry. Anesthesiology 93:947–953
25. Yoxall CW, Weindling AM 1998 Measurement of cerebral oxygen consumption in the human neonate using near infrared spectroscopy: cerebral oxygen consumption increases with advancing gestational age. Pediatr Res 44:283–290
26. Duncan A, Meek JH, Clemence M, Elwell CE, Fallon P, Tyszczuk L, Cope M, Delpy DT 1996 Measurement of cranial optical path length as a function of age using phase resolved near infrared spectroscopy. Pediatr Res 39:889–894
27. Altman DI, Perlman JM, Volpe JJ, Powers WJ 1993 Cerebral oxygen metabolism in newborns. Pediatrics 92:99–104
28. Brazy JE, Lewis DV 1986 Changes in cerebral blood volume and cytochrome aa3 during hypertensive peaks in preterm infants. J Pediatr 108:983–987
29. Wyatt JS, Cope M, Delpy DT, Richardson CE, Edwards AD, Wray S, Reynolds EO 1990 Quantitation of cerebral blood volume in human infants by near-infrared spectroscopy. J Appl Physiol 68:1086–1091
30. Brun NC, Greisen G 1994 Cerebrovascular responses to carbon dioxide as detected by near-infrared spectrophotometry: comparison of three different measures. Pediatr Res 36:20–24
31. Leung TS, Aladangady N, Elwell CE, Delpy DT, Costeloe K 2004 A new method for the measurement of cerebral blood volume and total circulating blood volume using near infrared spatially resolved spectroscopy and indocyanine green: application and validation in neonates. Pediatr Res 55:134–141
32. Sakai F, Nakazawa K, Tazaki Y, Ishii K, Hino H, Igarashi H, Kanda T 1985 Regional cerebral blood volume and hematocrit measured in normal human volunteers by single-photon emission computed tomography. J Cereb Blood Flow Metab 5:207–213
33. Powers WJ, Grubb RL Jr, Darriet D, Raichle ME 1985 Cerebral blood flow and cerebral metabolic rate of oxygen requirements for cerebral function and viability in humans. J Cereb Blood Flow Metab 5:600–608
34. Ballabh P, Braun A, Nedergaard M 2004 Anatomic analysis of blood vessels in germinal matrix, cerebral cortex, and white matter in developing infants. Pediatr Res 56:117–124
35. Wyatt JS, Cope M, Delpy DT, van der Zee P, Arridge S, Edwards AD, Reynolds EO 1990 Measurement of optical path length for cerebral near-infrared spectroscopy in newborn infants. Dev Neurosci 12:140–144
36. van der Zee P, Cope M, Arridge SR, Essenpreis M, Potter LA, Edwards AD, Wyatt JS, McCormick DC, Roth SC, Reynolds EO 1992 Experimentally measured optical pathlengths for the adult head, calf and forearm and the head of the newborn infant as a function of inter optode spacing. Adv Exp Med Biol 316:143–153
37. Duncan A, Meek JH, Clemence M, Elwell CE, Tyszczuk L, Cope M, Delpy DT 1995 Optical pathlength measurements on adult head, calf and forearm and the head of the newborn infant using phase resolved optical spectroscopy. Phys Med Biol 40:295–304
38. Ijichi S, Kusaka T, Isobe K, Islam F, Okubo K, Okada H, Namba M, Kawada K, Imai T, Itoh S 2005 Quantification of cerebral hemoglobin as a function of oxygenation using near-infrared time-resolved spectroscopy in a piglet model of hypoxia. J Biomed Opt 10:24026
39. Brun NC, Moen A, Borch K, Saugstad OD, Greisen G 1997 Near-infrared monitoring of cerebral tissue oxygen saturation and blood volume in newborn piglets. Am J Physiol 273:H682–H686
40. Kusaka T, Isobe K, Nagano K, Okubo K, Yasuda S, Kondo M, Itoh S, Hirao K, Onishi S 2002 Quantification of cerebral oxygenation by full-spectrum near-infrared spectroscopy using a two-point method. Comp Biochem Physiol A Mol Integr Physiol 132:121–132